ORIGINAL PAPER

Molecular modeling of the piezoelectric effect in the ferroelectric polymer poly(vinylidene fluoride) (PVDF)

Vladimir S. Bystrov · Ekaterina V. Paramonova · Igor K. Bdikin · Anna V. Bystrova · Robert C. Pullar · Andrei L. Kholkin

Abstract In this work, computational molecular modeling and exploration was applied to study the nature of the negative piezoelectric effect in the ferroelectric polymer polyvinylidene fluoride (PVDF), and the results confirmed by actual nanoscale measurements. First principle calculations were employed, using various quantum-chemical methods (QM), including semi-empirical (PM3) and various density functional theory (DFT) approaches, and in addition combined with molecular mechanics (MM) methods in complex joint approaches (QM/MM). Both PVDF molecular chains and a unit cell of crystalline β-phase PVDF were modeled. This computational molecular exploration clearly shows that the nature of the so-called negative piezo-electric effect in the ferroelectric PVDF polymer has a self-consistent quantum nature, and is related to the redistribution of the electron molecular orbitals (wave functions), leading to the shifting of atomic nuclei and reorganization of all total charges to the new, energetically optimal positions, under an applied electrical field. Molecular modeling and first principles calculations show that the piezoelectric coefficient d_{33} has a negative sign, and its average values lies in the range of $d_{33} \sim -16.6$ to -19.2 pC/N (or pm/V) (for dielectric permittivity $\varepsilon = 5$) and in the range of $d_{33} \sim -33.5$ to -38.5 pC/N (or pm/V) (for $\varepsilon = 10$), corresponding to known data, and allowing us to explain the reasons for the negative sign of the piezo-response. We found that when a field is applied perpendicular to the PVDF chain length, as polarization increases the chain also stretches, increasing its length and reducing its height. For computed value of $\varepsilon \sim 5$ we obtained a value of $d_{31} \sim +15.5$ pC/N with a positive sign. This computational study is corroborated by measured nanoscale data obtained by atomic force and piezo-response force microscopy (AFM/PFM). This study could be useful as a basis for further insights into other organic and molecular ferroelectrics.

Keywords Molecular models · Piezoelectric effects and coefficients · Polymer ferroelectrics · PVDF

V. S. Bystrov (✉) · R. C. Pullar · A. L. Kholkin
Department of Materials Engineering and Ceramics & CICECO,
University of Aveiro, 3810-193 Aveiro, Portugal
e-mail: bystrov@ua.pt

V. S. Bystrov
e-mail: vsbys@mail.ru

V. S. Bystrov · E. V. Paramonova
Institute of Mathematical Problems of Biology RAS,
142290 Pushchino, Moscow region, Russia

I. K. Bdikin
Centre for Mechanical Technology and Automation (TEMA),
University of Aveiro, 3810-193 Aveiro, Portugal

A. V. Bystrova
Institute of Biomedical Engineering and Nanotechnology,
Riga Technical University, LV-1658 Riga, Latvia

Introduction

Piezoelectricity in polyvinylidene fluoride (PVDF) is well known, and has been investigated by many authors [1–16]. Nevertheless, the nature of the piezoelectric effect, especially for the "negative piezoelectric effect" in these PVDF materials is still not clear, although several attempts have been made to solve this problem [10–16]. The usual approaches were based on several theoretical assumptions and simplifications, necessary to construct the models with corresponding Hamiltonian and equations, which must be then solved correctly. The results obtained by these methods permit the description of the experimental data by several different approximations. However, the major question is still unanswered — why do these molecular organic polymers demonstrate a negative piezoelectric response

in several directions, while in others it is positive? Which is the cause and nature of these phenomena?

In this paper we report our results on the direct first principles studies, modeling and calculations of optimized molecular models for the PVDF molecular chain, as well for the lattice unit cell of the PVDF β−phase crystal state. We perform the optimization of the total energy of the system, and as a result we have established new geometrical positions for each atom, and their corresponding physical parameters and properties, which lead directly to the negative piezoelectric reaction of the system in the perpendicular to chain direction. We perform these calculations mainly by the semi-empirical quantum-mechanical (QM) PM3 method, using HyperChem 7.5 and 8.0 [17]. We also involve several density functional theory (DFT) methods for more precise ab initio calculations, and molecular mechanics (MM) methods for the optimization of the largest molecular system models in combination with QM methods. The main principle is the search for the total energy minimum, with corresponding reorganization of all parts of the system to new atomic positions, charges and bond lengths. This results in new system parameters and determines new properties under an applied field, from which arise a negative piezoelectric response and a negative value for the piezoelectric coefficient, d_{33}. Finally, the computed data are compared with experimental data obtained by atomic force and piezoresponse force microscopy (AFM/PFM) techniques, and the results are analyzed to explain the features of this experimental data.

Computational details

In this work, several versions of molecular models for PVDF ferroelectrics were developed and investigated using HyperChem 7.52 as well as 8.0 [17]. We studied the dependence of the main PVDF electrical properties (dipole momentum, polarization, atomic charges and bond lengths, energies of electron subsystems as well as the total energy of the systems), both without and under an applied electrical field. We explored molecular models of PVDF ferroelectrics with different lengths of the molecular chain, and for a unit cell of the PVDF crystal lattice in the β-phase.

Various computational methods were used, including molecular mechanics (MM) methods (such as BIO CHARM [17]), quantum mechanical (QM) self-consistent field (SCF) Hartree-Fock (HF) calculations based on density functional theory (DFT), as well as semi-empirical methods (such as PM3), in both restricted Hartree-Fock (RHF) and unrestricted Hartree-Fock (UHF) approximations. The main approach of both the MM and (QM) methods used for molecular modeling is to obtain the minimum of the total,

or potential energy surface (PES), of a studied molecular system. The optimization of molecular geometry is executed using the Polak–Ribere (conjugate gradient) algorithm, which determines an optimized geometry at the minimum energy point (using PES) [17].

The MM methods do not treat electrons explicitly. The electron subsystem and electron charges are described only by quantum wave functions. The QM calculation methods expand molecular orbitals of calculated molecular structures into linear combinations of atomic orbitals (LCAOs) for electron wave functions. The DFT method computes the electron density by integrating the square of the wave function, and uses it in all further calculations. Semi-empirical methods differ mainly in the treatment of electron–electron interactions, and by using parameterization approaches.

In our previous comparable study of these approaches to PVDF and similar structures, which was published recently [18], we showed the reasonable validity of the semi-empirical PM3 method in this case. In these studies we used various DFT methods, which are accessible in the HyperChem package, such as many-parameter exchange-correlation functional method HCTH98 (by Handy et al. [19]), Becke-88 functional [20] with Lee-Yang-Parr (LYP) correlation functional [21], and Perdew-Wang-91 exchange functional [22] in combination with the fastest and most suitable PM3 semi-empirical method [17, 18]. It is well known that both DFT approaches and the semi-empirical methods are widely used, and have developed very rapidly [23, 24], but each have their own strengths and weaknesses. Because of this, it is an important practice to consider the most effective combinations of these different approaches.

PM3, developed by Stewart [25], is based on the so-called "neglect of diatomic differential overlap (NDDO)" approximation, with several modifications and with the choice of a wide number of parameters to reproduce experimental quantities. For PVDF, the most accurate HF calculations are based on the HF Hamiltonian of the full molecular system, with valence double electron wave-functions including correlation interactions on d-polarization functions for C and F atoms, and p-polarization functions for H atoms. However, using DFT calculations for our PVDF system with a higher level of accuracy usually required a very long time and a large amount of computer memory. PM3 generally is the most accurate and rapid QM computational method, utilizing several experimental parameters to simplify the calculation process [25]. Therefore, we tried to compare the calculated data with faster and simpler semi-empirical quantum-chemical methods, such as PM3 approximation.

PM3 is based on NDDO approximation with a special choice of parameters. For example, the core-core repulsion

integral, or the interaction energy between the nuclei A in the quantum mechanical region and the charges B (including the nuclear charges and the electronic charges) could be described by the following relationship [17, 25, 26]:

$$\Delta E_N(A, B) = \sum_{(A,B)} \left\{ Z_A Z_B(s_A s_A | s_B s_B) \left[1 + e^{-\alpha_A R_{AB}} + \frac{e^{-\alpha_A R_{AB}}}{R_{AB}} \right] - Z_A Q_B(s_A s_A | s_B s_B) \right\}, \tag{1}$$

with parameterization of two-centers $(s_A s_A | s_B s_B)$ integrals, e.g., in the following form [17]

$$(s_A s_A | s_B s_B) = \frac{1}{\left[R_{AB}^2 + \frac{1}{2} \left(\frac{1}{AM_A} + \frac{1}{AM_B} \right)^2 \right]^{1/2}}, \tag{2}$$

where Z_A, Z_B are the nuclear charges, R_{AB} is the distance between them, Q_B is the net charge (the nuclear charge minus the electron charge) on atom B, and AM are the monopole-monopole interaction parameters.

PM3, especially in the UHF approximation, is the most suitable and quickest method for the calculation of the total charge redistribution (under quantum interactions including redistribution of all electron wave functions) and polar properties, for molecular polymers, such as PVDF, consisting of carbon, hydrogen and fluorine atoms. For the more complex cases, we used a combination of PM3 with MM methods such as BIO CHARM, which is more suitable for calculations of such polymer systems. In this work, for testing and comparing results at a more precise level, we also used DFT methods (included in HyperChem [17]), but the main used is PM3. The precise DFT methods need much more time and computer memory, but in combination with the faster and suitable PM3 semi-empirical method, they give the best practical results. It is important in practice to exploit the effective combinations of these different computational approaches.

Molecular models: results and discussion

Model of initial structure and electric field application

We consider the model of the PVDF crystal structure to be that presented in Fig. 1a. We use the standard well known cell parameters for the initial state of this PVDF structure: the lattice constants of the used hexagonal symmetry unit cell are a=0.858 nm (8.58 Å), b=0.491 nm (4.91 Å), c=0.256 nm (2.56 Å) [1–10] (Fig. 1b, c). We can think of parameter a as being in the direction of the chain width, b as in the direction of the chain height, and c as in the direction of the chain length. After an optimization of total energy is performed for the

modeled systems, these parameters are changed for each special case, as described and shown below.

We construct the PVDF chain with a length of 12 monomer units ($C_2H_2F_2$), and on one end of chain we also add half a unit (total length is 12.5 units) for a better symmetry in the modeled system (Fig. 2). From our previous studies, we know that more than 6–10 monomer units are enough for accurate calculations [7–9]. Then, we select the central part, with one unit cell (Fig. 1b, c); and then select one PVDF chain from the most stable, central part of this, as shown in Fig. 2. For all these models and their selected parts, we calculate all necessary parameters using the quantum-chemical semi-empirical method PM3. Firstly, we calculate the initial states and all parameters of the PVDF system without an electrical field, taking into detailed consideration the central part of this one PVDF chain, as shown in Fig. 2.

The coordinate's origin is placed on the central atom (marked as C0, see Figs. 1c and 2) with the OX axis directed from the zero point and to the right, and the OZ axis from the zero point and in an upward direction (perpendicular to the main PVDF chain axis). We determine the main computed data for this part — the coordinates of each atom, bond lengths and atomic charges (as shown in Fig. 2). Then, we apply an electrical field $E = E_z$ in the OZ axis (using a special option in HyperChem), directed along the dipole moment of the PVDF chain (Fig. 3). The value and sign of E_z were varied, and all calculations (with evaluation of the self-consistent geometry optimization of the total system's energy under an applied electric field) were repeated again with each change in electrical field values.

Deformation of molecular chain and individual dipole under influence of applied electric field

The main results of this modeling and calculations are the following (see Figs. 4a, b and 5a, b) — this is after the application of an electrical field with a sign corresponding to the positive OZ direction along the PVDF chain's total dipole moment. There is an initial rise of the dipole value, and the chain experiences deformation consisting of a reduction of the chain height h ($h1$ and $h2$ in the central part), with a corresponding increase in the total PVDF chain length l, as the chain effectively stretches along its length.
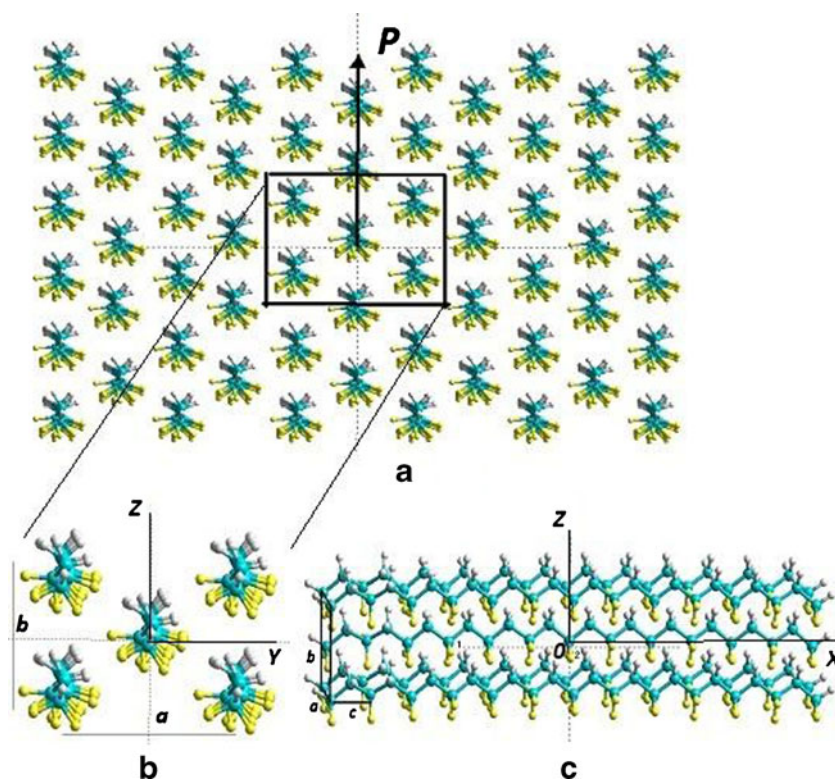
As a result, the total PVDF polarization is raised, while the total system energy decreases, with an increase of electric field value in the OZ direction (Fig. 6a). These data correspond to the negative electrostriction and negative piezoelectric effect in the OZ direction (in accordance with electromechanical coupling in ferroelectrics [27]). If the electric field increases in the opposite direction to the total dipole of the chain and corresponding polarization, when it reaches

some critical value (the coercive field, E_c) the PVDF chain is rotated into the opposite orientation of dipoles with respect to applied electric field (Fig. 6b). These important cycling peculiarities of the PVDF energy hysteresis loop could serve for further applications in energy harvesting and storage systems [27].

More detailed exploration allows us to conclude that each individual dipole ($C_2H_2F_2$) rotates under an applied

Fig. 2 Molecular model of PVDF chain with symmetrized 12.5 monomer units with total length equal *l* along OX axis, and presentation of PVDF chain with enlarged image of the central part; schematic of the main parameters studied — sizes and charges of the most stable central part of PVDF chain's skeleton: distances *h1* and *h2* — heights of chain along OZ axis at the C1 and C2 positions, c1 and c2 — chain distances between C0-C3 and C0-C4 atoms, bond lengths a1, a2, a3, a4 and charges C0, C1, C2, C3, C4, H1, H11, H2, H21, F1, F2, F31, F41 and F42
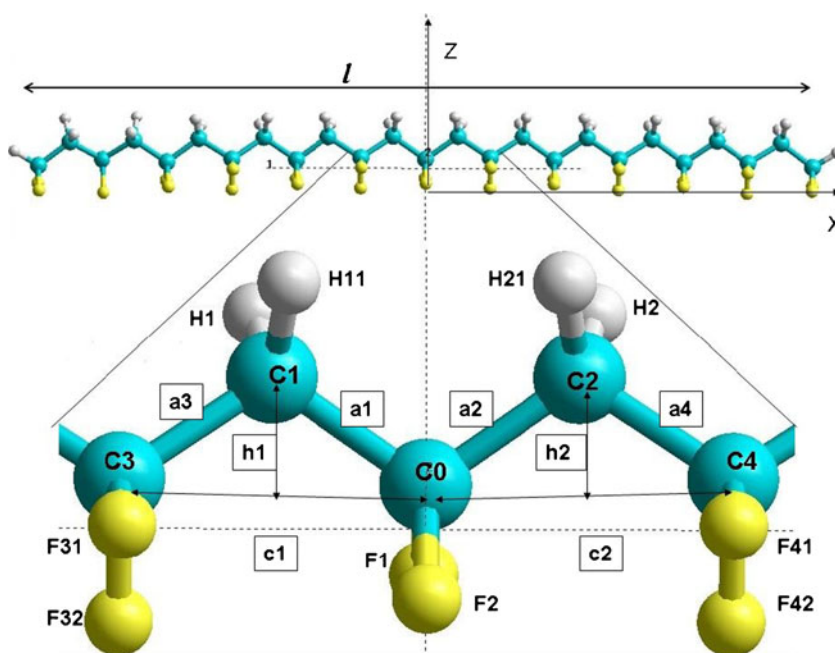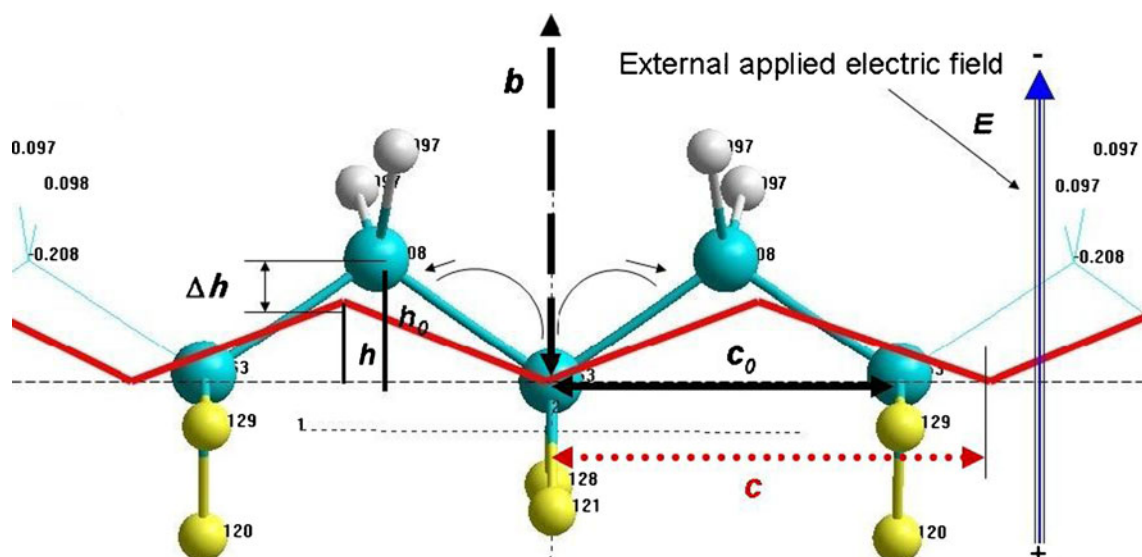
Fig. 3 Schematic of the electric field application on the PVDF chain, and the deformation of one segment of the PVDF chain's skeleton under an external applied electric field: orientation of electric field along PVDF total dipole moment axis OZ (*red line* — schematic of PVDF chain's skeleton deformation); deformation of PVDF chain's skeleton height h in the direction of electric field along vertical OZ axis: $\Delta h = h0 - h$, ($h0$ — initial state); the height h is directed along unit cell parameter b, initial unit cell parameter along chain is c_0, and c is this parameter after deformation. All marked and numbered atoms are the same as in Fig. 2

electrical field and changes its orientation. Moreover, neighboring dipole pairs rotate in an opposite direction, which leads to a change of the angles of the PVDF chain skeleton and further leads to a total chain deformation in a similar manner to a spring, along with its "negative" height reaction to an applied electrical field. All these actions are illustrated schematically in Fig. 7. These features of PVDF chain behavior in an applied electrical field are following from the common energy minimum principle — because we optimize the geometry and search for the minimum of the total system energy at each step of the calculations. As a result, it is shown that total energy is decreasing with an increase in electric field in OZ direction for this case, and a corresponding rise of total dipole moment and polarization of PVDF (Fig. 6).

Polarization switching, hysteresis loop and coercive field

Further exploration of these models and calculations show that, in the case when the electrical field has a sign with opposite orientation to the dipole, it leads to a decrease of the total dipole moment of the PVDF chain, and an increase of the chain skeleton height with corresponding decrease of its length. The total energy in this case increases, but only up to a critical value, after which the optimization of energy leads to the fast chain rotation into the opposite direction, along with the chain's total dipole momentum. The chain's dipole now coincides again with the electric field direction, and is manifested in an energy jump to a new minimal value. Such behavior leads to the known hysteresis loop and

switching phenomena for the PVDF chain's total dipole momentum, as well as its polarization (see in Supplementary information Fig. S1a) and energy (Fig. 6b), which is in agreement with our earlier calculations [7, 8, 28] and allows us to estimate the value of the coercive electric field $E_c \sim 0.005$ a.u. (~ 2.5 GV/m), and a corresponding coercive voltage $V_c \sim 0.22$ V (for average $h \sim 0.88$ Å). As for deformation, for the variation in height of the chain's skeleton, we obtain a "butterfly" plot of this switching (see in Supplementary information Fig. S1b), which corresponds to all known data for PVDF materials. These calculated results are compared qualitatively with the experimental data (see in Supplementary information Fig. S3).

Calculation of the piezoelectric coefficient from model for changes in the height of the chain

Of great interest is the direct calculation of the piezoelectric coefficient, d_{33} in this case. For this purpose, we must recalculate the value of the electric field and distance (height h of chain skeleton in this case) to obtain the corresponding voltage value for each of these distances (model with using h). Such a recalculation is presented in Table 1 for the h_1 data set, and in Table 2 for the h_2 data set. As a result, we obtain the set of d_{33} values and its average value $<d_{33}>$. The calculated average values of our data are $<d_{33}>=-16.3$ pC/N (for $\varepsilon=5$) and -32.6 pC/N (for $\varepsilon=10$) in the case of a PVDF height change of h_1, and $<d_{33}>=-22.2$ pC/N (for $\varepsilon=5$) and -44.4 pC/N (for $\varepsilon=10$) in the case of height h_2 (see data in Tables 1 and 2).
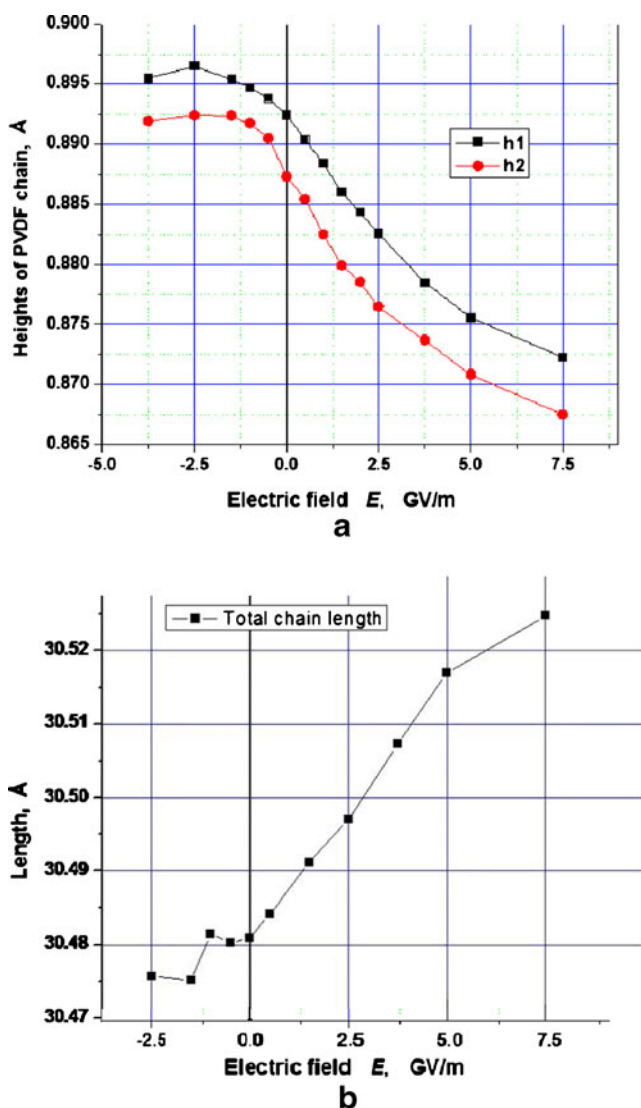
Fig. 4 Computed data on changes of the main PVDF chain's skeleton sizes under applied electrical field, demonstrated its different deformations: **a** Changes of heights of the skeleton in the central part (see Figs. 2 and 3), showing its decreases with electric field rise ("negative" deformation). **b** Change of total length of PVDF chain consisting from 12.5 units, which is risen with electric field increase ("positive" deformation)
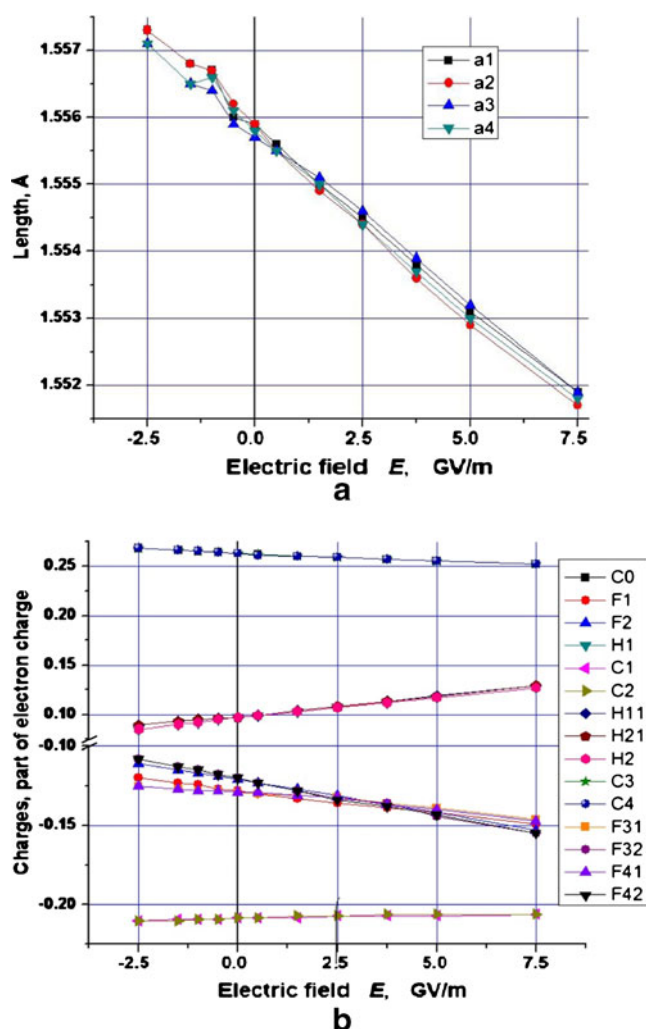

Fig. 5 Parameters of the PVDF chain's skeleton with electric field alteration (see Fig. 2): **a** Bond lengths between carbon atoms in the central part of the PVDF chain. **b** Charges of atoms in the central part of the PVDF chain's skeleton. Total sum of all atoms charges vary very small around zero value: Qs=0.014 (E=0), Qs=0.035 (E=−2.5 GV/m), Qs=−0.005 (E=2.5 GV/m), Qs=−0.027 (E=5 GV/m)

The total average values for both h_1 and h_2 are $<d_{33}>=-19.3$ pC/N (for $\varepsilon=5$) and $<d_{33}>=-38.5$ pC/N (for $\varepsilon=10$) (see below data in Table 2). These results correspond closely to many of the known theoretical and experimental data [10–16]; for example, the data for d_{33} from [15] is $d_{33}=-25.2$ pC/N, from [16] is $d_{33}=-33$ pC/N, and from [10] is $d_{33}=-38$ pC/N. This last value is for P(VDF-TrFE) at 295 K, not for pure PVDF, but it is still close to our results. (We plan to compute P(VDF-TrFE) too).

We have estimated the statistical errors and deviations for all these cases, using standard statistical analysis with a 95 % probability confidence level (Tables 1 and 2).

The data show that for an applied electric field $E=E_z>0$, the spread of deviations from average values is low, in the

order of 1–2 %, while for $E=E_z<0$ the deviations are much greater, in the order of 5–20 %. This situation could be additionally illustrated by the behavior of the chain height with applied electric field, as presented in Fig. 4a. This clearly shows that with an increasing negative field the behavior of the height of the polymer chain becomes very complex and ambiguous. This is understandable, because it can be seen that we are approaching a point of bifurcation at the critical electric field value — the coercive field. However, for the sake of completeness, we conducted a full final averaging of the values of the piezoelectric coefficient. By this point, this error has reached almost 50 %, but nevertheless the average data were quite comparable with the known values. We finally codified all the results and present them in comparison with other data in Table 4.
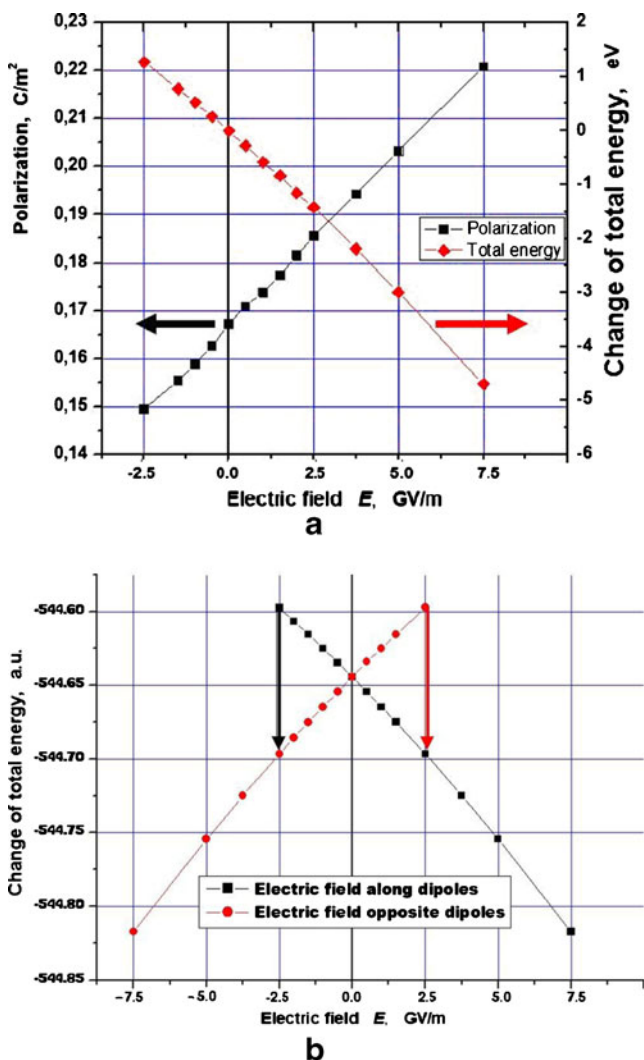
Fig. 6 Electric field influence: **a** Changes of the total PVDF chain polarization and the total energy of this system under increasing applied electrical field, $E = Ez$, along the OZ axis, which is corresponding to the main PVDF chain dipole orientation. **b** Energy hysteresis and switching of energy corresponding to the PVDF chain rotation into the opposite orientation, with respect to the applied electric field

The main impact of the proposed model is that it can explain directly from the first principle calculations the reasons for the "negative" values of the piezoelectric effect and d_{33} in PVDF. It follows directly from the energy minimum principle for the behavior of this total dipole system under an applied electric field, which leads to the "negative piezoelectric effect", and explains that the nature of such behavior arises from the molecular "spring" properties of each molecular PVDF chain. Therefore, it is clearly shown that the nature of such "negative" reactions are the self-consistent quantum redistribution of electron molecular orbitals (wave functions), leading to the shifting of atomic charged nuclei and the reorganization of all total charges to the new energetically optimal positions in an applied electrical field.

Calculation of piezoelectric coefficient from the model of unit cell parameter *b*

To further strengthen the results of our models and approaches, we also considered a more detailed model. This was for the full central unit cell and the deformation of the cell parameter *b*, which is the chain height, oriented in the OZ direction, parallel with and opposite to the applied electrical field E_z, and perpendicular to the length of the chain. This is a very complicated case for direct quantum calculation, involving full energy optimization of the total system energy, and in this case we used a combination of the PM3 method with molecular mechanics calculations using BIO CHARM, for total energy calculation at the applied electric filed values, and with variation of the inter-chain distance (changing the cell parameter, *b*). Moreover, we can not use the optimization calculation in this case as well, because we have a "cluster" geometry with "surface", but not an infinite crystal with repeated unit cells as in local-density approximation (LDA) and DFT calculations [23, 29]. Optimization leads to additional "surface" deformation of our cluster in this case. For correct calculation we can use only the single point (SP) for each fixed atomic position. However, we can change the distance *b* at each step of the calculation, and calculate the total energy for this unit cell structure by the BIO CHARM method. Firstly, we determine each chain's energy, charges and bond length by PM3. Such a combined approach allows us to obtain the dependence of our unit cell model's total energy on electric field, and find the minimum of energy for this system.

An example of such calculations of total energy for this case, at two different values of the electric field, is shown in Fig. S2 (see in Supplementary information). We found that the minimum energy points in these models shifted with an opposite sign to the applied electric field, as can also be seen in Table 3, e.g., increasingly positive applied fields led to a decrease in *b*. Table 3 also shows that d_{33} (and average $<d_{33}>$) is <0, and all these d_{33} values are very close to those above, that we obtained for one PVDF chain, as well as to previously published PVDF data (see for example data in [13, 30, 31]). The obtained data changes in lattice constant *b* and its average values are in the range of $<d_{33}>=-18.87$ pC/N for $\varepsilon=5$, and $<d_{33}>=-37.73$ pC/N for $\varepsilon=10$ (see the data in Table 3). Therefore, these results confirm the data, and the nature of the molecular behavior for PVDF chains, as well as for a whole PVDF unit cell. The statistical errors were also calculated (see Table 3), and the computed data is also presented in Table 4 (as our second d_{33} model, "using *b*")

The findings of our exploration into the origin of the "negative" piezoelectric modulus in PVDF are confirmed by many other authors' results and data [10–17], who tried to obtain theoretical expressions for piezoelectricity in similar polymers. For example, both Broadhurst et al. [12] and
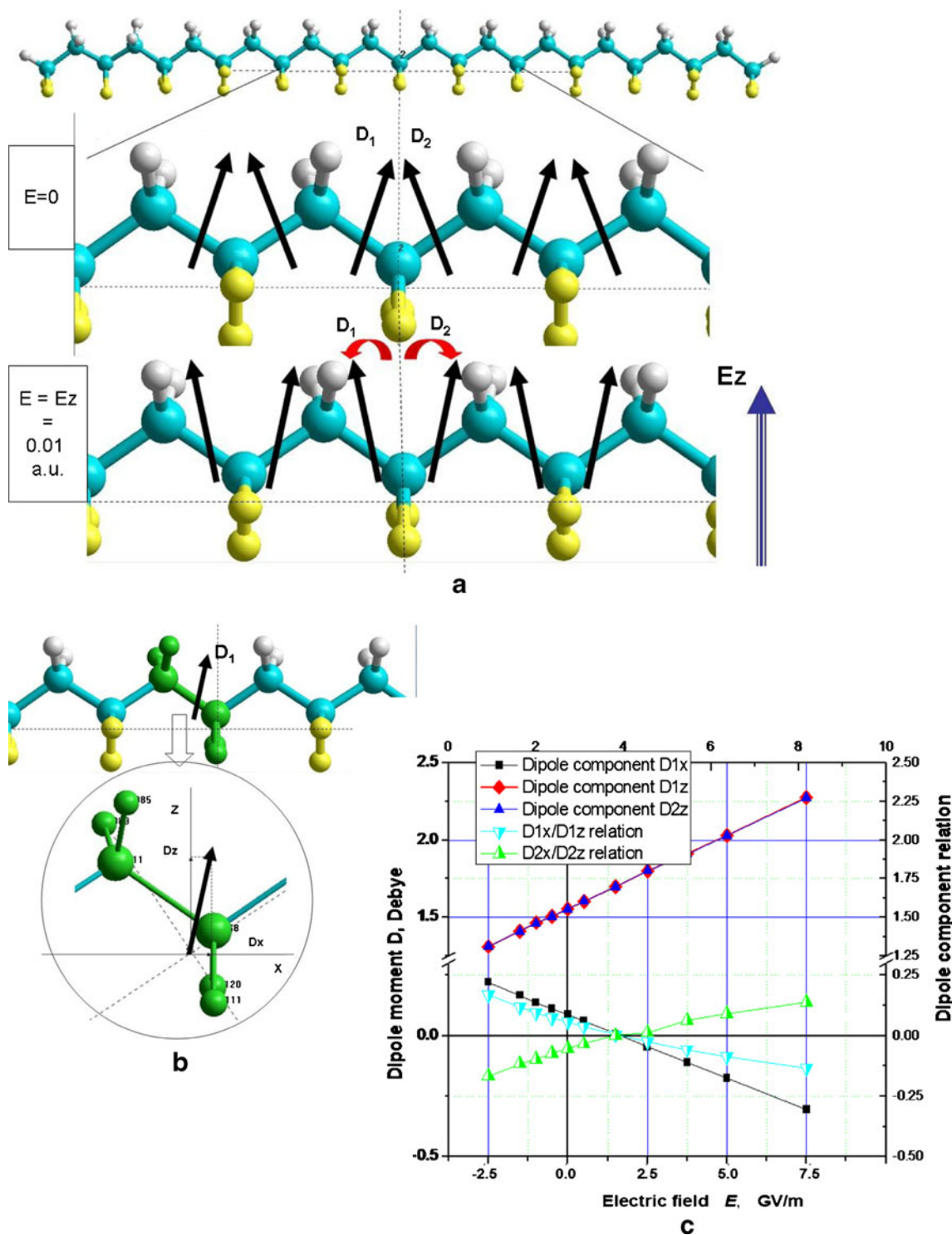
Fig. 7 Schematics of partial rotations of individual monomer's dipoles under an applied electric field along the OZ direction: **a** Left and right unit dipoles of the central PVDF skeleton part, without (*E*=0) and under an applied electric field, *E*=Ez=0.01 a.u~5 GVcm. **b** One selected unit dipole (*green*) with the dipole components shown. **c** Changes of unit dipole components and their relationships under an applied electric field in the OZ direction (along the main dipole orientation)

Wada et al. [11] had considered the so-called "dimensional effect" as the origin of such negative piezoelectricity in organic ferroelectrics. They proposed that dipoles in polymers were rigid, molecular dipoles that retained a fixed moment and orientation during the mechanical deformation of samples, and any piezoelectric response was attributed to macroscopic dimensional changes. A similar approach was taken by Omote et al. [10], which involved the influence of

Table 1 Calculated data for piezoelectric coefficients from changes in height of the PVDF chain, under an applied electrical field along the vertical OZ direction, together with total PVDF dipole moment orientation, and the corresponding voltage changes at each distance of PVDF height at the position **h1** in Figs. 2 and 4

#	E appl., a.u., (1 a.u. ~ 500 GV/m)	h1, Å	U, V	Δh1, Å	$d_{33} = \Delta h_1/U$, pm/V = pC/N		
					$\varepsilon=1$	$\varepsilon=5$	$\varepsilon=10$
1	0.0150	0.87227	0.672520	−0.02014	−2.994710	−14.9735	−29.94706
2	0.0100	0.87558	0.437790	−0.01683	−3.844310	−19.2216	−38.44309
3	0.0075	0.87849	0.338658	−0.01392	−4.110340	−20.5517	−41.10343
4	0.0050	0.88256	0.226820	−0.00985	−4.342650	−21.7133	−43.42651
5	0.0040	0.88439	0.181831	−0.00802	−4.410700	−22.0535	−44.10699
6	0.0030	0.88598	0.136620	−0.00643	−4.706480	−23.5324	−47.06485
7	0.0020	0.88841	0.091329	−0.00400	−4.379790	−21.899	−43.79791
8	0.0010	0.89038	0.045770	−0.00203	−4.435220	−22.1761	−44.3522
9	0	0.89241	0	0			
	Average 1					-20.765	-41.53
	St. error 1[a]					±2.22	±4.34
10	0	0.89241	0	0			
11	−0.0010	0.89378	−0.04594	0.00137	−2.982150	−14.9108	−29.82151
12	−0.0020	0.89472	−0.09198	0.00231	−2.511550	−12.5578	−25.11548
13	−0.0030	0.89542	−0.13808	0.00301	−2.179900	−10.8995	−21.79896
14	−0.0050	0.89649	−0.23040	0.00408	−1.770830	−8.8516	−17.70829
	Average 2					−11.805	−23.611
	St. error 2[a]					±2.44	±4.87
	Average 12					−16.285	−32.57
	St. error 12[a]					±3.30	±6.52

[a] Statistical error at the probability 95 % for confidence level of standard deviation

the intrinsic piezoelectric effect arising mainly from the inclination of dipoles on applying external stress, while they also included the influence of the dimensional effect appearing due to lattice deformation by external strain, without changing the dipole orientation. This last result implies that the contribution of the intrinsic piezoelectric effect is comparable to the dimensional effect [10]. Purvis and Taylor have made the classical continuum approximation for a crystal lattice unit cell model, and calculated similar negative values for d_{33} [13, 30]. However, in our molecular model approach we do not make any similar theoretical assumptions — it is direct, self-consistent quantum calculation of the molecular model from the first principle quantum-chemical positions. We only constructed the molecular model of our ferroelectric polymer chain from a series of individual dipoles (and then the following crystal lattice unit cell model made from the same molecular chains). Then we carried out the total energy optimization, both without and under the influence of an external electric field, applied along and opposite the direction of the main dipole orientations of the PVDF molecular chain. This effect arises from a complex cooperative movement of all of the molecular PVDF chain dipoles, which is one of the main properties of ferroelectric materials. The result is a complex deformation in the common chain skeleton, as well for each individual monomer dipole unit, and for all bond lengths and charges. This causes an effective stretching along the chain length (the OX axis), finally leading to an average negative piezoelectric response in the perpendicular OZ axis (in the molecular chain as well as in the lattice unit cell), and a negative value of d_{33}.

Calculation of the piezoelectric coefficient using electromechanical coupling

Using our computed data for a direct estimation of the electrostriction deformation, s, under an applied electric field, we can also obtain the value of the electrostriction coefficient $Q \sim s/P^2$, where P is our computed polarization ($P\sim0.17$ C/m^2 for E=0 from these our data), an s is the deformation under the action of an applied electric field. For the case of one PVDF chain, we estimate the value of s, from the change of the chain's height from our data, to be $s = \Delta h/h \sim -0.019$. This corresponds to a calculated value of the electrostriction coefficient $Q \sim -(0.7–1.0)$ m^4/C^2, comparable with known data for PVDF of $Q \sim -(2.0–2.4)$ m^4/C^2

Table 2 Calculated data for piezoelectric coefficients from changes of height of the PVDF chain, under an applied electrical field along vertical OZ direction, together with total PVDF dipole moment orientation, and corresponding voltage changes at each distance of PVDF height at the position **h2** in Figs. 2 and 4

#	E appl., a.u., (1 a.u. ~ 500 GV/m)	$h2$, Å	U, V	$\Delta h2$, Å	$d33 = \Delta h_2/U$, pm/V = pC/N		
					$\varepsilon=1$	$\varepsilon=5$	$\varepsilon=10$
1	0.0150	0.86748	0.668829	−0.01983	−2.964880	−14.8244	−29.64885
2	0.0100	0.87084	0.447612	−0.01647	−3.679500	−18.3975	−36.795
3	0.0075	0.87371	0.336815	−0.01360	−4.037030	−20.1852	−40.37028
4	0.0050	0.87650	0.225261	−0.01081	−4.798900	−23.9945	−47.98899
5	0.0040	0.87856	0.180632	−0.00875	−4.844100	−24.2205	−48.44103
6	0.0030	0.87993	0.135685	−0.00738	−5.439730	−27.1987	−54.3973
7	0.0020	0.88247	0.090718	−0.00510	−5.632850	−28.1642	−56.32846
8	0.0010	0.88544	0.045510	−0.00187	−4.109030	−20.5451	−41.09027
9	0	0.88730	0	0			
	Average 1					−22.191	−44.383
	St. error 1[a]					±3.69	±7.39
10	0	0.88730	0	0			
11	−0.0010	0.89053	−0.04577	0.003220	−7.035180	−35.1759	−70.35176
12	−0.0020	0.89175	−0.09167	0.004440	−4.843460	−24.2173	−48.4346
13	−0.0030	0.89237	−0.13760	0.005060	−3.677330	−18.3866	−36.77326
14	−0.0050	0.89240	−0.22935	0.005090	−2.219320	−11.0966	−22.19316
	Average 2					−22.2191	−44.438
	St. error 2[a]					±9.60	±19.3
	Average 12					−22.205	−44.4105
	St. error 12[a]					±10.3	±19.6
	Average total h1h2					−19.245	−38.49
	St. error h1h2[a]					±10.5	±20.3

[a] Statistical error at the probability 95 % for confidence level of standard deviation

[32, 38]. In the case of cell deformation along the **b** direction, we obtain a similar value: $s \sim \Delta b/b \sim -0.028$ and $Q \sim -1.1$ m⁴/C². Moreover, we estimated the polarizability from our computed data of the dipole moment and polarization changes under an electric field, and found the computed value of the polarizability for PVDF chain. We calculated polarizability to be $\alpha_0 \sim 34$ Å³ ~

Table 3 Calculated data for piezoelectric coefficients from changes of height of the PVDF chain, under an applied electrical field along vertical OZ direction, together with total PVDF dipole moment orientation, and corresponding voltage changes at each value of PVDF cell unit parameter **b** (Fig. 1). Value of **b** corresponds to the minimum point of total energy distribution for each electric field value (see examples in Supplementary information Fig. S2), obtained by SP calculations with the BIO CHARM method, with **b** parameter alteration, after PM3 optimization of each PVDF chain for a five chain unit cell model (Fig. 1)

#	E appl., a.u., (1 a.u. ~ 500 GV/m)	b, Å	U, V	$\Delta b = (b-b_0)/2$, Å	$d_{33} = \Delta b/U$, pm/V=pC/N		
					$\varepsilon=1$	$\varepsilon=5$	$\varepsilon=10$
1	0.0150	4.83	3.72393	−0.09	−2.41680	−12.084	−24.1680
2	0.0100	4.87	2.50318	−0.07	−2.79645	−13.98225	−27.9645
3	0.0050	4.91	1.26187	−0.05	−3.96195	−19.80975	−39.6195
4	0.0030	4.95	0.76329	−0.03	−3.93035	−19.65175	−39.3035
5	0	5.01					
6	−0.0020	5.07	−0.5212	−0.03	−5.75599	−28.77995	−57.5599
	Average					−18.86154	−37.72308
	St. error[a]					±5.8	±11.8

[a] Statistical error at the probability 95 % for confidence level of standard deviation

Table 4 Piezoelectric properties of PVDF, calculated in this work, and data collected from previous references

	This work			P&T[a]		Bune[b]	Nix[c]	Markus[d]	O&O[e]	Tashiro[f]
	Method	ε=5	ε=10	calc	exp					
d_{33}, pC/N	using **h**	−19.2	−38.5	−21.4	−31.5	−20				
	using **b**	−18.9	−37.7	−28.9	−33.3		−33	−39	−38	−25.2
	Eq. (3)	−16.6	−33.5			−32				
d_{31}, pC/N	similar to Eq. (3)	15.5		18.3	21.4		16.5	24	7	

[a] Ref [13] (two various models used ε=4, polarization P=0.086 C/m^2, different exp.)

[b] Ref [29] (first data exp., second by Eq. (3), used ε=8, polarization P=0.1 C/m^2)

[c] Ref [16]

[d] Ref [30] (with ε=15)

[e] Ref [10]

[f] Ref [15]

$3.8*10^{-39}$ C*m^2/V for one chain, which corresponds well to known data [8, 28, 33] and α~328 Å^3~$36.5*10^{-39}$ C*m^2/V for a unit cell model made from five chains. We also estimated the value of dielectric permittivity, ε, following the Clausius-Mossotti relation in a similar manner to that used in [27, 33, 34]. The obtained value is ε~2.2 for the one chain model, that again corresponds to similar data [33], and is in range of ε~4.65 … 5 for the unit cell model made from five chains, which is very close to known experimental data [3–16, 18, 28, 30, 32] . These data allow us to determine the value of the piezoelectric coefficient d_{33} through an approximate relation of electromechanical coupling [27, 34–36]:

$$d_{33} = 2Q\varepsilon\varepsilon_0 P \qquad (3)$$

These directly calculated data clearly show again the same ranges of d_{33} values as the modeled data obtained above: for the PVDF cell model the calculated data are d_{33}~−16.55 to −33.5 pC/N (or pm/V) over the dielectric permittivity range of ε~5 to 10. All these data are in good agreement with our estimations above (computed by other approaches, which additionally confirms their validity), as well as with known data from literature [1–16, 27, 28, 30–33, 37, 38]. While the calculated statistical errors (see Table 3) in this case are some of the largest (this could be explained because it is the most complex model and computational approach), compared to the two previous approaches, nevertheless it has reasonable agreement with known data. All data is collected in Table 4.

An additional estimation was made for the piezoelectric coefficient in the longitudinal direction along the PVDF chain, corresponding to the piezoelectric coefficient d_{13}. Taking into account the fact that the chain length along the OX axis increases as an electric field applied along the OZ axis (see Fig. 4b), and using the results to estimate that Q~1 m^4/C^2 and ε~5, we calculate that the value of d_{31}~15.5

pC/N (or pm/V) with a positive sign, which is in good agreement with the known data [10, 13, 30, 38].

It is likely that for other molecular dipole systems, similar results could be modeled and calculated, because those dipole systems should reach an energy minimum point under similar conditions. This suggests that such behavior must be common to other molecular and organic ferroelectrics. We will continue this study into other related systems.

Finally, we want to emphasize that this model allows us to explain the observed nanoscale behavior of PVDF during PFM measurements, reported in our previous work [39], and the observed "dark" and "bright" images. The "dark" section in this case directly corresponds to a "negative" piezoelectric effect as the PVDF chain's skeleton **h** goes down and unit cell parameter **b** is decreased (decrease in height), and the "bright" section to a "positive" effect following the opposite rising deformation of the chain height **h** and cell width **b**, in response to an applied electric field in the opposite direction (see in Supplementary information Fig. S3a). For a more detailed and accurate quantitative comparison of measured and computed data, such as the hysteresis loop and butterfly-plot shown in Fig. S1 and Fig. S3 (see Supplementary information), there needs to be further study and an improvement of the models, of course. More experimental and computational details are presented in [35, 36]. However, the proposed model describes very well the qualitative comparisons of the system's behavior.

The peculiarities of PVDF's behavior under an applied electric field, especially changes in energies such as those shown in Fig. 6, would be more pronounced when in the vicinity of a phase transition, when conformation changes (e.g., from trans to gauche PVDF chain conformations) can occur under (induced by) an electric field [40]. This could open up new opportunities for high speed energy harvesting and storage systems based upon PVDF and its copolymers.

These questions are in progress and will be discussed in more detail in the next article by the authors.

Conclusions

This computational molecular exploration clearly shows that the nature of the so-called negative piezo-electric effect in the ferroelectric PVDF polymer has a self-consistent quantum character, which is connected with the redistribution of electron molecular orbitals, the shifting of charged atomic nuclei, and complex cooperative dipole reorganization in the bonded molecular chain, under the action of applied electrical field. The resulting complicated non-uniform and nonlinear anisotropy deformation of the PVDF molecular chain, arising from both individual interacting and chemically bonded dipoles of $C_2H_2F_2$, as well as from the PVDF unit cell, leads to negative deformation in relation to the applied field (OZ axis). This causes an affective stretching of the chain length and compression of chain height, when a field is applied perpendicular to the PVDF chain, leading to a reduction in the b lattice parameter. Molecular modeling and first principles calculations (by various methods) allow us to obtain the average values of the piezoelectric coefficient, d_{33} in this case, which has a negative sign and lies in the range of $d_{33}\sim-16.6$ to -19.2 pC/N (or pm/V) (for $\varepsilon=5$) and in the range of $d_{33}\sim-33.5$ to -38.5 pC/N (or pm/V) (for $\varepsilon=10$). This corresponds to known data, and allows us to explain the reasons for the negative sign of the piezo-response. Additionally, it was possible to explain the nature of the "dark" and "bright" images of the PFM signal. As expected, the value of d_{31} is approximately $d_{31}\sim15.5$ pC/N (or pm/V) with a positive sign. This study could be useful for further insight into other organic and molecular ferroelectrics, and it could be a base for possible new applications of this negative piezoeffect on the nanoscale.

References

1. Tashiro K (1995) In: Nalwa HS (ed) Ferroelectric polymers. Dekker, New York, pp 63–181
2. Furukawa T (1989) Phase Transit 18:143–211
3. Bune AV, Fridkin VM, Ducharme S, Blinov LM, Palto SP, Sorokin AV, Yudin SG, Zlatkin A (1998) Nature 391:874–877
4. Blinov L, Fridkin V, Palto S, Bune A, Dowben P, Ducharme S (2000) Physics-Uspekhi 43:243–257
5. Qu H, Yao W, Zhang J, Dusharme S, Dowben PA, Sorokin AV, Fridkin VM (2003) Appl Phys Lett 82:4322–4324
6. Kliem H, Tardos-Morgane R (2005) J Phys D: Appl Phys 38:1860–1868
7. Bystrov V, Bystrova N, Paramonova E, Sapronova A (2006) Ferroelectr Lett 33:153–162
8. Bystrov VS, Bystrova NK, Paramonova EV, Vizdrik G, Sapronova AV, Kuehn M, Kliem H, Kholkin AL (2007) J Phys Condens Matter 19:456210
9. Bystrov VS, Paramonova EV, Dekhtyar Y, Katashev A, Polyaka N, Bystrova AV, Sapronova AV, Fridkin VM, Kliem H, Kholkin AL (2011) Math Biol Bioinforma 6(2):t14–t35, http://www.matbio.org/2011/Bystrov2011(6_t14).pdf
10. Omote K, Ohigashi H, Koga K (1997) J Appl Phys 81(6):2760–2769
11. Wada Y, Hayakawa R (1981) Ferroelectrics 32:115–118
12. Broadhurst MG, Davis GT, McKinney JE, Collins RE (1978) J Appl Phys 49:4992. doi:10.1063/1.324445
13. Purvis CK, Taylor PL (1983) J Appl Phys 54(2):1021–1028
14. Furukawa T, Wen JX, Suzuki K, Takashina Y, Date M (1984) J Appl Phys 56:829. doi:10.1063/1.334016
15. Tashiro K, Kobayashi M, Tadokoro H, Fukada E (1980) Macromolecules 13:691–698
16. Nix EL, Ward IM (1986) Ferroelectrics 67:137–141
17. HyperChem (2002) Tools for molecular modeling (release 7, 8) professional edn. Hypercube Inc, Gainesville http://www.hyper.com/?tabid=360
18. Bystrov VS, Paramonova EV, Dekhtyar Y, Pullar RC, Katashev A, Polyaka N, Bystrova AV, Sapronova AV, Fridkin VM, Kliem H, Kholkin AL (2012) J Appl Phys 111:104113. doi:10.1063/1.4721373
19. Hamprecht FA, Cohen AJ, Tozer DJ, Handy NC (1998) J Chem Phys 109:6264. doi:10.1063/1.477267
20. Becke AD (1988) Phys Rev A 38:3098–3100
21. Johnson BG, Gill PM, Pople JA (1993) J Chem Phys 98:5612-5627 doi:10.1063/1.464906
22. Perdew JP, Chevary JA, Volsko SH et al. (1992) Phys Rev B 46:6671–6687
23. Zhao Y, Truhlar DG (2007) Acc Chem Res 41(2):157–167
24. Stewart JJP (2008) J Mol Model 14:499–535
25. Stewart JJP (1989) J Comput Chem 10:209–220, 221–264
26. Stewart JJP (2007) J Mol Model 13:1173–1213
27. Lines ME, Glass AM (1977) Principles and applications of ferro-electrics and related materials. Clarendon, Oxford
28. Bystrov VS, Bystrova NK, Kiselev D, Paramonova EV, Kuehn M, Kliem H, Kholkin AL (2008) Integr Ferroelectr 99(1):31–40
29. Briddon PR, Jones R (2000) Phys Status Solidi B-Basic Res 217:131–171
30. Kepler RG, Anderson RA (1978) J Appl Phys 49:4490. doi:10.1063/1.325454
31. Zhu G D, Zeng Z G, Zhang L, Yan X (2008) Comp Mater Sci. doi:10.1016/j.commatsci.2008.03016
32. Newnham RE, Sundar V, Yimnirun R, Su J, Zhang QM (1997) J Phys Chem B 101:10141–10150
33. Yamada K et al (2001) Jpn J Appl Phys 40:4829–4836
34. Hereida A, Bdikin I, Kopyl S, Mishina E, Semin S, Sigov A, German K, Bystrov V, Gracio J, Kholkin AL (2010) J Phys D: Appl Phys 43:462001
35. Bdikin IK, Bystrov VS, Kopyl S et al (2012) Appl Phys Lett 100:043702. doi:10.1063/1.3676417
36. Bdikin I, Bystrov V, Delgadillo I, Grasio J, Kopyl S, Wojtas M, Mishina E, Sigov A, Kholkin AL (2012) J Appl Phys 111:074104
37. Bune AV, Zhu C, Ducharme S, Blinov LM, Fridkin VM, Palto SP, Petukhova NG, Yudin SG (1999) J Appl Phys 85:7869. doi:10.1063/1.370598
38. Marcus MA (1982) Ferroelectrics 40:29–41
39. Bystrov VS, Bdikin IK, Kiselev DA, Yudin SG, Fridkin VM, Kholkin AL (2007) J Phys D: Appl Phys 40:4571–4577
40. Ranjan V, Nadelli MB, Bernholc J (2012) Phys Rev Lett 108:087802